Eur. Phys. J. B **33**, 9–14 (2003)
DOI: 10.1140/epjb/e2003-00135-2

THE EUROPEAN PHYSICAL JOURNAL B

Interface phonon assisted transition in double quantum well

B.H. Wu[1,a], J.C. Cao[1], G.Q. Xia[1], and H.C. Liu[2]

[1] State Key Laboratory of Functional Materials for Informatics, Shanghai Institute of Microsystem and Information Technology, Chinese Academy of Sciences, 865 Changning Road, Shanghai 200050, PR China
[2] Institute for Microstructural Sciences, National Research Council, Ottawa, Ontario K1A 0R6, Canada

Received 22 December 2002
Published online 23 May 2003 – © EDP Sciences, Società Italiana di Fisica, Springer-Verlag 2003

Abstract. A detailed calculation of interface phonon assisted electron intersubband transition in double GaAs/AlGaAs quantum well structure is presented. Our calculation concentrates on the lowest two subbands which can be designed to be in resonance with a given interface phonon mode. Various phonon mode profiles display quasi-symmetric or quasi-antisymmetric shapes. The quasi-antisymmetric phonon modes give rise to much larger transition rates than those assisted by quasi-symmetric ones. The transition rate reaches a maximum when the subband separation coincides with a given phonon mode energy. The calculation procedure presented here can be easily applied to the design and simulation of other low dimensional semiconductor structures, such as quantum cascade lasers.

PACS. 78.67.De Quantum wells – 63.20.Kr Phonon-electron and phonon-phonon interactions – 72.10.Di Scattering by phonons, magnons, and other nonlocalized excitations

1 Introduction

The teraherz (THz) electromagnetic spectral region has recently attracted much attention due to its applications in imaging, communication, astronomy and biological sensing. Several new ideas have been proposed to produce THz radiation [1–9]. The remarkable success of THz intersubband quantum cascade lasers (QCL) has been recently reported [6,7]. Central to the intersubband based THz devices is the phonon assisted transition and carrier relaxation. Phonon assisted transitions should be designed to maximize the population inversion [10,11]. It has been shown that the electron phonon scattering rates may be dominated by interface phonons for the case where quantum well confinement dimensions are less than about 50 Å [10]. It is then desirable to band engineer quantum well parameters to allow interface phonon assisted transitions to occur and to maximize their rates. This is the key point to achieve a lowest lasing threshold. A new structure to produce THz radiation by optical pumping in double quantum wells (DQW) has been demonstrated recently [8,9]. In the DQW three-level system, electrons emit THz ratiation when the population inversion between the second and the third subbands is achieved. The interface phonon assisted transition is believed to play an important role in the lasing process.

In this article, we carry out calculations of subbands in GaAs/AlGaAs DQW using Schrödinger equation coupled with Poisson equation [12]. The interface LO phonon modes in the dielectric continuum model are used in the Fermi golden rule to evaluate intersubband transition rates. Our results show that the DQW parameters and interface phonon potential profiles can greatly influence the transition rates.

[a] e-mail: bhwu@263.net

2 Electron states in quantum well structures

The eigen-energies and wave functions for electrons in the quantum well structures are obtained by solving the Schrödinger equation with an appropriate Hamiltonian. Neglecting many body interactions among electrons, the one-electron Hamiltonian is used to describe the electron motion in a DQW structure. Choosing the z coordinate as the quantum well direction, the one-electron Schrödinger equation in the effective mass approximation is written as

$$-\frac{\hbar^2}{2}\frac{\mathrm{d}}{\mathrm{d}z}\frac{1}{m^*(z)}\frac{\mathrm{d}}{\mathrm{d}z}\phi(z)+V(z)\phi(z)=E\phi(z), \quad (1)$$

where $\phi(z)$ is the envelope wave function, $\hbar$ is the Plank's constant divided by 2π, $m^*(z)$ is the effective mass near the conduction band edge, which is constant in the well or barrier region, E is the z component of the energy, and $V(z)$ is the total potential energy,

$$V(z)=V_{\text{built-in}}(z)-|e|V_F(z), \quad (2)$$

where $V_{\text{built-in}}(z)$ is the built-in potential energy, and $-|e|V_F(z)$ is the net electrostatic potential energy due to

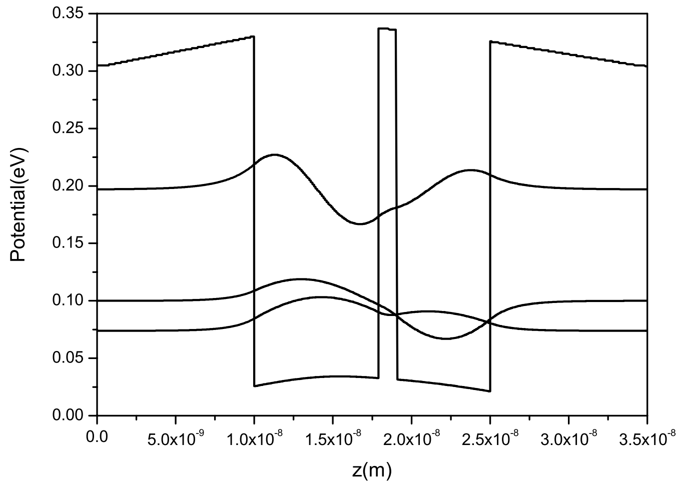

Fig. 1. Self-consistently calculated DQW structure potential profile and the lowest three subband wavefunctions. The two GaAs well widths are 73 Å and 60 Å. The AlGaAs barrier width is 11.3 Å. The modulation doping is placed 100 Å away from the DQW. The total electron density is 3×10^{11} cm^{-2}.

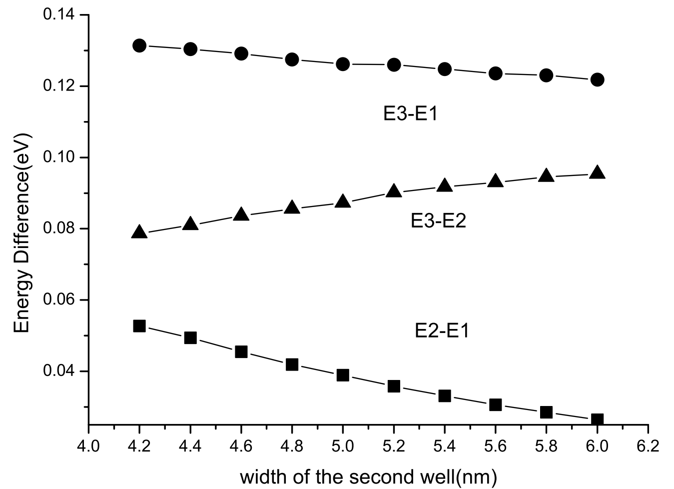

Fig. 2. Energy spacings between subbands as a function of the second well width. The first well and the barrier width are fixed at 79 Å and 11.3 Å.

screening effect. $V_F(z)$ is obtained by solving the Poisson equation with an appropriate charge distribution inside the quantum well. Self-consistent calculations are required to take into account the screening effect. $V_F(z)$ satisfies the following Poisson equation,

$$\frac{\mathrm{d}}{\mathrm{d}z}\left(\epsilon(z)\frac{\mathrm{d}}{\mathrm{d}z}\right)V_F(z) = -|e|[N_D(z) - N_A(z) + p(z) - n(z)], \quad (3)$$

in which $\epsilon(z)$ is the dielectric constant, $N_D(z)$ and $N_A(z)$ are the densities of donors and acceptors, respectively, and $p(z)$ and $n(z)$ are the densities of holes and electrons, respectively. The boundary conditions are $V_F(z) = 0$ at the quantum well boundaries (without an applied electric field). For an n-type modulation doped quantum well, $N_D(z) \gg N_A(z)$ and $n(z) \gg p(z)$ are assumed, and $N_A(z)$ and $p(z)$ are neglected in solving the Poisson equation.

For the ith subband, the density $n_i(z)$ at position z equals the electron surface concentration in the ith subband N_{is}, multiplied by $|\phi_i(z)|^2$. The total electron density $n(z)$ is the sum of the densities in all subbands:

$$n(z) = \sum_i n_i(z) = \sum_i N_{is}|\phi_i(z)|^2. \quad (4)$$

The band nonparabolicity effect of the effective mass is taken into account by the Kane-type dispersion [13]. The self-consistent calculations are performed to solve the wave function, subband energy, potential profile and carrier distribution. Figure 1 shows the resulting DQW total potential and the lowest three subband wavefunctions. The calculated example of the asymmetric DQW structure, similar to those investigated experimentally [9], consists of two GaAs quantum wells separated by $Al_{0.35}Ga_{0.65}As$ barriers. The GaAs well widths are 79 Å and 60 Å, respectively. The barrier between the two wells is 11.3 Å. Two modulation doping spikes are placed at 100 Å away from the DQW. The total electron density is 3×10^{11} cm^{-2}.

With the widths of the first well and the barrier fixed, the energy separation between the subbands can be tailored by changing the width of the second well. Figure 2 shows the relation between subband separation and the well width. We can easily select the proper well width to make the first two subbands in resonance with a given interface phonon mode.

3 Interface phonon modes in quantum well structures

In theoretical treatments of electron-LO-phonon interactions in heterostructures, both macroscopic [14] and microscopic [15] approaches have been employed. The electrostatic potentials and dispersion relations of interface phonons in the DQW structure are determined by the transfer matrix method [16]. Interface phonon modes are characterized by exponentially decaying amplitudes away from a heterointerface. The frequencies of these modes depend on the type of materials used in the heterostructure and the number of the modes depends on the number of interfaces in the structure. The electrostatic potentials of interface phonon modes are linear combinations of exponentially-growing and exponentially-decaying spatial functions. The form of the interface phonon mode along the growth direction in any given layer is expressed as

$$\Phi_i(q, z) = A_i \mathrm{e}^{-qz} + B_i \mathrm{e}^{+qz}, \quad (5)$$

where q is the phonon wave vector in the in-plane direction. If there are n interfaces of alternating binary and ternary materials (such as the structure we study here), there are $3n$ interface modes. Since there are four interfaces in the DQW structure, we find 12 interface phonon

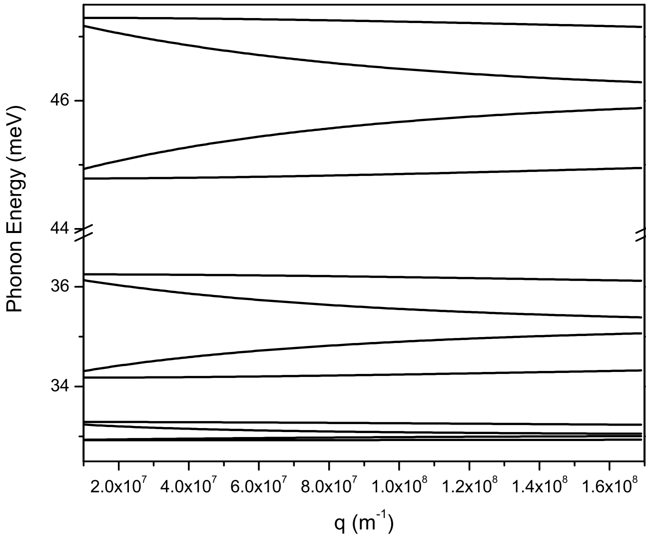

Fig. 3. The interface phonon dispersion relation calculated for the DQW structure. The two GaAs quantum wells have well widths of 79 Å and 52 Å. The AlGaAs barrier width is 11.3 Å. 12 interface modes due to the four heterointerfaces in the structure are shown.

modes. The phonon potential as well as the tangential component of the electric field have to be continuous across each heterointerface. For example at the interface of the ith and $(i+1)$th layer, the electrostatic potential should satisfy the following equations,

$$\Phi_i(q,z) = \Phi_{i+1}(q,z), \tag{6}$$

$$\epsilon_i \frac{\partial}{\partial z}\Phi_i(q,z_i) = \epsilon_{i-1}\frac{\partial}{\partial z}\Phi_{i-1}(q,z_i). \tag{7}$$

Following the Lyddane-Sachs-Teller relation, the dielectric function ϵ_i can be written as follows. For a binary compound semiconductor:

$$\epsilon_i(\omega) = \epsilon_i(\infty)\frac{\omega^2-\omega_{LO}^2}{\omega^2-\omega_{TO}^2}, \tag{8}$$

and for a ternary compound semiconductor:

$$\epsilon_i(\omega) = \epsilon_i(\infty)\frac{(\omega^2-\omega_{LOA}^2)(\omega^2-\omega_{LOB}^2)}{(\omega^2-\omega_{TOA}^2)(\omega^2-\omega_{TOB}^2)}. \tag{9}$$

The transfer matrix method [16] is used to compute the phonon frequencies as well as the mode electrostatic potential profiles. The dispersion relation is obtained by requiring the phonon potential to vanish when $z=\pm\infty$. Detailed descriptions of this method as well as dielectric constants and phonon frequencies are found in reference [16]. Figure 3 shows the calculated results. There are eight GaAs-like modes having energies from 32 to 37 meV (four lower GaAs-like modes and four upper GaAs-like modes), and four AlAs-like around 46 meV. The normalization of the potential of each interface phonon mode is given by

$$\frac{\hbar}{2\omega} = \sum_i \frac{\epsilon_0}{2\omega}\frac{\partial\epsilon_i(\omega)}{\partial\omega}\int_{R_i}\mathrm{d}z\left(q^2|\Phi_i(q,z)|^2 + \left|\frac{\partial\Phi_i(q,z)}{\partial z}\right|^2\right). \tag{10}$$

The amplitude of phonon mode potential can be determined from this relation. Electrostatic potentials for the interface phonon modes in DQW are plotted in Figure 4. Since the DQW structure is asymmetric, the phonon potentials do not possess exact parities. Strictly speaking, these modes cannot be categorized as symmetric or antisymmetric interface modes. For convenience and as an approximation, we separate them into quasi-symmetric and quasi-antisymmetric modes according to the signs of the potential in the two wells. If the signs of a mode are the same, we call this mode quasi-symmetric; and the opposite is true for a quasi-antisymmetric mode. In each panel of Figure 4, there are two quasi-symmetric interface phonon modes and two quasi-antisymmetric ones. We will see that the quasi-antisymmetric modes give rise to much larger scattering rates than the quasi-symmetric modes.

4 Phonon assisted intersubband transition rates

The phonon induced transition rate between two electronic states $|n,k\rangle$ and $|n',k'\rangle|$ is given by Fermi's golden rule,

$$W_{n,n'}^{\binom{a}{e}}(k,k') = \frac{2\pi}{\hbar}|\langle n'k', N_q \pm 1|H_{e-ph}|nk, N_q\rangle|^2 \times \delta(E_{n'}+E_{k'}\pm\hbar\omega - E_n - E_k) \tag{11}$$

where E_n and $E_{n'}$ are the band-edge energies of the nth and n'th subbands, k and k' are the in-plane wave vectors of the initial and final states, respectively, $E_k=\hbar^2k^2/2m$ is the in-plane energy, ω is the frequency of a given phonon mode, and N_q is the phonon population following Bose-Einstein statistics. The superscripts e and a denote emission and absorption processes, respectively. The energy and momentum are conserved during the transition process. When the subband separation is smaller than the phonon energy, an electron emitting a phonon has to possess some in-plain energy. The two dimensional in-plane wave vector conservation relation can be written as $k = k' + q$. Due to energy conservation, some transitions are forbidden. For the emission process, when $E_k < \hbar\omega' \equiv \hbar\omega - (E_n - E_{n'})$ and $\omega' > 0$, *i.e.*, the two subband edges are closer than a phonon energy and the electron does not posses enough initial kinetic energy, there are then no final states available and the process is forbidden. For $\omega' > 0$ and $E_k > \hbar\omega$ the interface phonon assisted emission rate can be written as [10,17]

$$W_{n,n'}(k) = \frac{1}{4\pi^2}\frac{2\pi}{\hbar}(N_q+1)\int_{-\theta_{max}}^{\theta_{max}}\mathrm{d}\theta\frac{2m}{\hbar^2} \times\frac{|F(q_+)|^2q_+ + |F(q_-)|^2q_-}{|q_+-q_-|}, \tag{12}$$

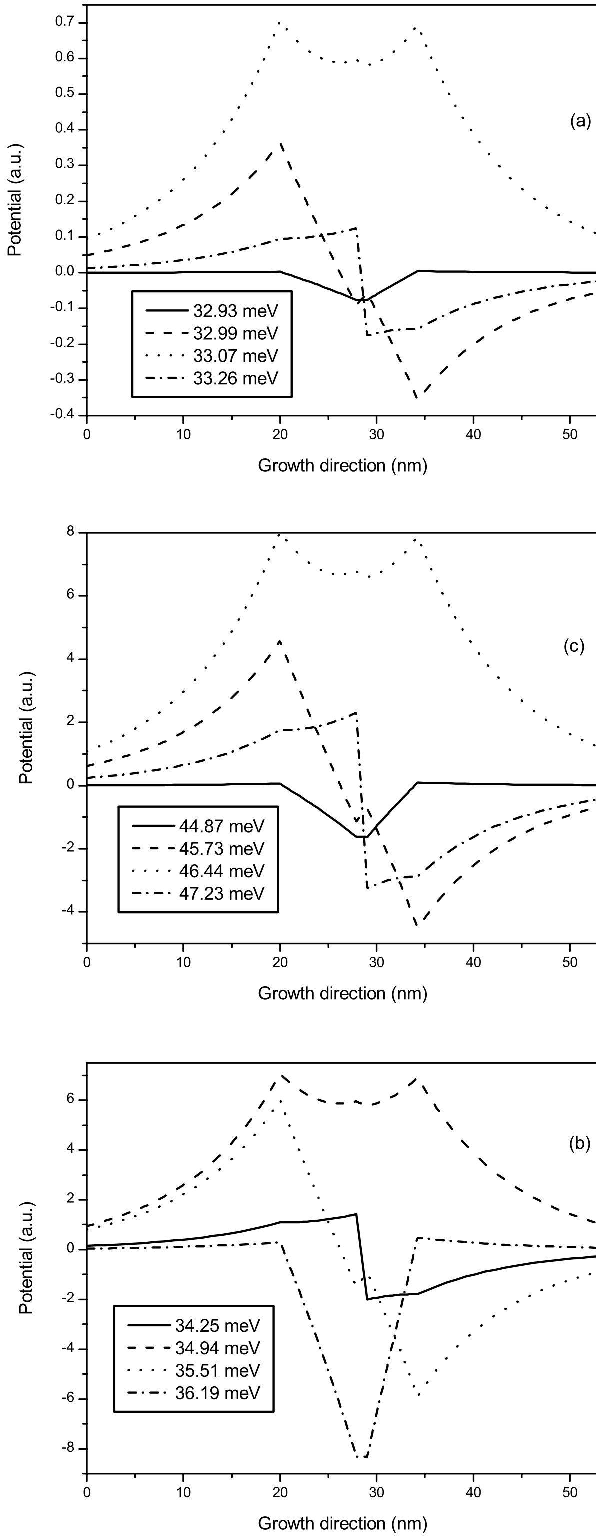

Fig. 4. Electrostatic potential for the interface phonon modes in the DQW structure: (a) lower GaAs-like interface phonon modes, (b) upper GaAs-like phonon modes, and (c) AlAs-like phonon modes. The parameters of the DQW structure are GaAs (79 Å)-AlGaAs (11.3 Å)-GaAs (52 Å). For this plot q is set to be $1.0 \times 10^8 \mathrm{m}^{-1}$. The corresponding phonon energy for each mode is shown in each panel.

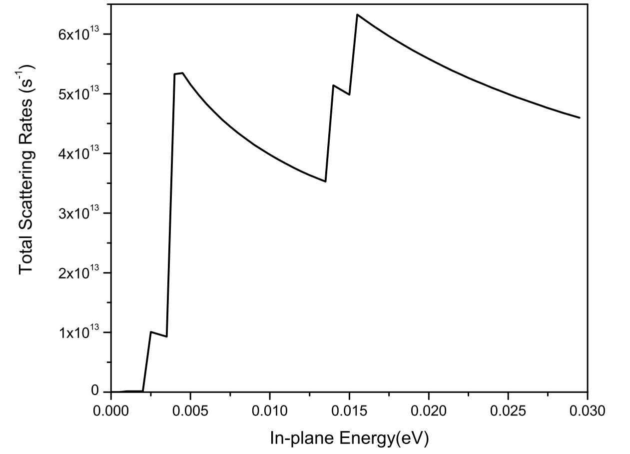

Fig. 5. Scattering rate for interface phonon modes. The structure parameters are 79 Å–11.3 Å–54 Å. The contributions from the quasi-antisymmetric modes are more evidence than the quasi-symmetric modes.

where

$$F(q) = -\int \mathrm{d}ze\phi(z)\psi_n^*(z)\psi_{n'}(z), \tag{13}$$

$$q_\pm = k\cos(\theta) \pm \sqrt{k^2\cos^2\theta - \frac{2m}{\hbar}\omega'}, \tag{14}$$

$$\theta_{max} = \cos^{-1}\left(\sqrt{\frac{2m\omega'}{\hbar k^2}}\right), \tag{15}$$

For $\omega' < 0$

$$W_{n,n'}(k,q) = \frac{1}{4\pi^2}\frac{2\pi}{\hbar}(N_q+1)\int_0^{2\pi}\mathrm{d}\theta\frac{2m}{\hbar^2}|F(q_+)|^2. \tag{16}$$

For the absorption process, similar expressions can be deduced under the same assumptions.

Only the emission rates are calculated here and are shown in Figure 5. From Figure 5, we can see that only several modes have dominant effects on the interface phonon modes assisted scattering rates. These modes are quasi-antisymmetric modes. Their potentials have the opposite sign in the two wells. Due to the parity consideration, the transition rates for the symmetric modes are zero in a symmetric structure. Since our DQW structure is asymmetric, each mode has its own contribution to the transition rates. Our calculation shows that the quasi-symmetric mode and quasi-antisymmetric mode contribute quite differently to the phonon assisted intersubband transition. In Figures 6 and 7, we will consider two interface phonon modes separately. One is the quasi-antisymmetric mode which has the largest scattering rates of all the interface modes, the other one is the quasi-symmetric modes which has a phonon energy close to that of the quasi-antisymmetric one. Let the two well widths of the DQW structure be 79 Å and L, where L is varied. The barrier width is 11.3 Å. The profile of the phonon mode at the energy of 36.19 meV has the same sign in the two wells – quasi-symmetric. Its potential

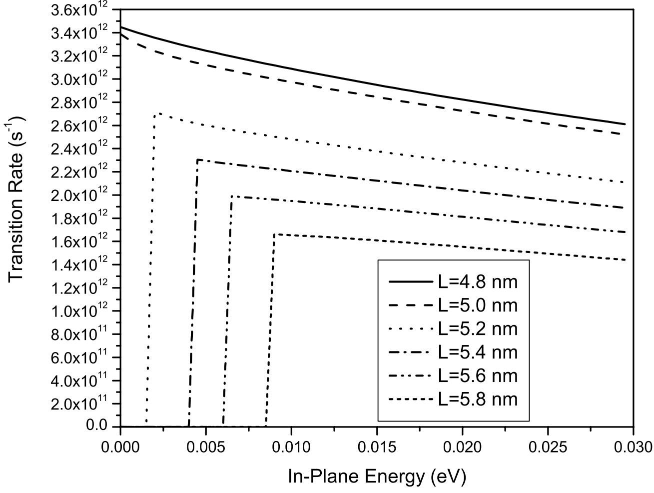

Fig. 6. Comparison of the transition rates for different well widths. The first well and the barrier width is fixed at 79 Å and 11.3 Å. Only the second well width (L) is varied. Only one quasi-symmetric phonon mode is considered in the calculation.

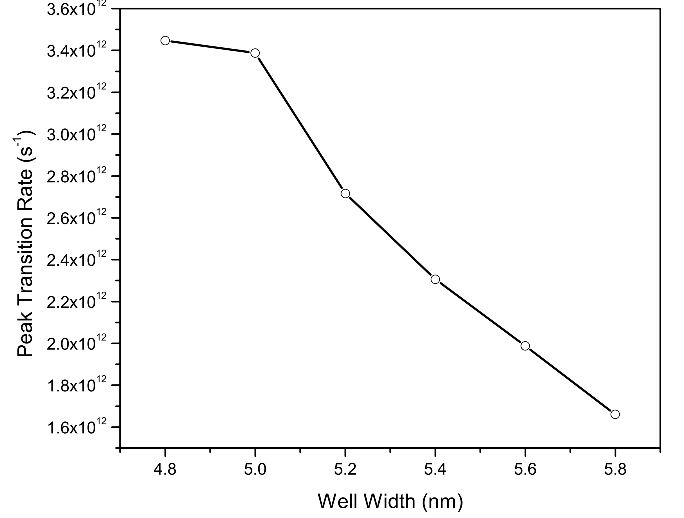

Fig. 8. Peak transition rate as a function of the second well width for the quasi-symmetric phonon mode. The structure parameters are the same as Figure 5.

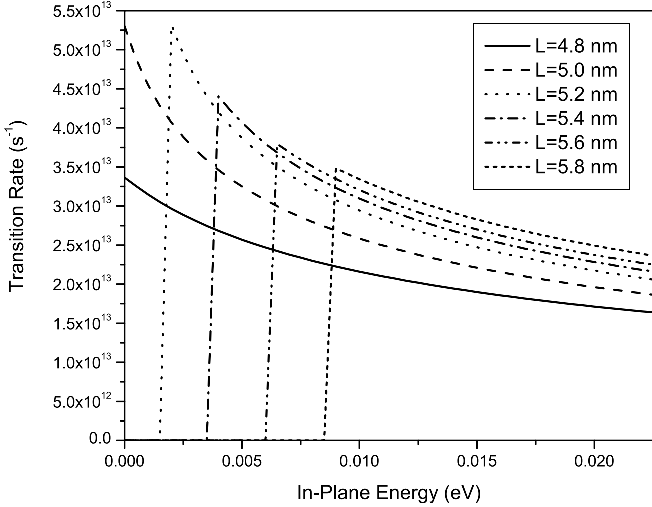

Fig. 7. Comparison of the transition rates for different well widths. The situation is the same as the former one, but the phonon mode considered here is a quasi-antisymmetric one. The quasi-antisymmetric phonon assisted transition rate is about an order of magnitude larger that assisted by the quasi-symmetric phonon mode.

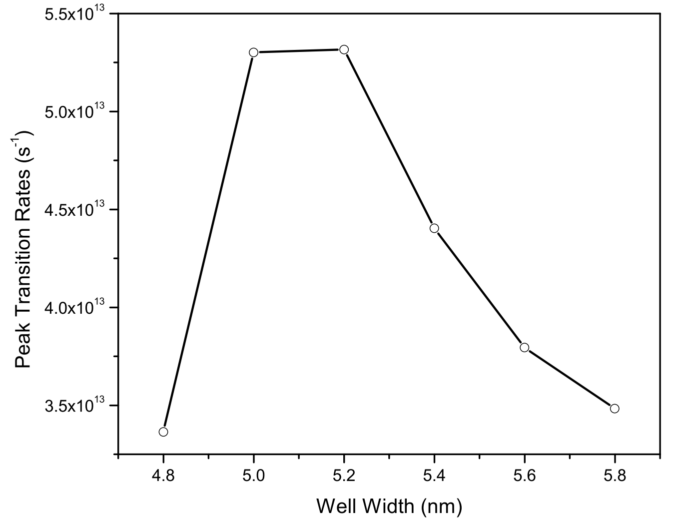

Fig. 9. Peak transition rate as a function of the second well width for the quasi-antisymmetric phonon mode. The structure parameters are the same as Figure 6. Note the enhancement when the phonon energy matches the subband separation.

profile can be found in Figure 4. Intersubband transition rates assisted by this mode is calculated. When L is varied from 48 Å to 58 Å, keeping all other parameters fixed, the calculated transition rate is shown in Figure 6. The same calculation is done for a quasi-antisymmetric mode at 35.51 meV. The result is shown in Figure 7. Comparing these results we find that the quasi-antisymmetric phonon assisted transition rate is significantly larger than that for the quasi-symmetric mode. This is reasonable considering the quasi-symmetric and quasi-antisymmetric shapes of the ground and the first excited state envelope functions. When the second well width is made to equal the first, the structure becomes symmetric. The quasi-symmetric and quasi-antisymmetric modes now become exactly symmetric and antisymmetric, respectively. The parity selection rule takes effect. The symmetric interface phonon assisted intersubband transition is now exactly forbidden and the antisymmetric interface phonon mode dominates the scattering process. In our structure, the role of quasi-symmetric interface phonon mode is expected to be weaker compared with quasi-antisymmetric mode. Our result agrees well with this consideration. This effect is also displayed in the peak transition rate as a function of the second well width (Figs. 8 and 9).

The peak transition rate is defined as the maximum value of transition rates as a function of the in-plane energy. The quasi-antisymmetric interface phonon assisted transition rates are about one order of magnitude larger than those for the quasi-symmetric interface phonons. Note the enhancement in the intersubband scattering rate when the subbands are exactly $\hbar\omega$ apart. The quasi-antisymmetric interface phonon mode is resonant when the second well width is between 50 Å to 52 Å aaccording to Figure 2. The result in Figure 9 exactly shows this conclusion. The quasi-symmetric interface phonon mode however displays no obvious resonance in Figure 8. In the device design, we should concentrate on the quasi-antisymmetric mode since it gives rise to the main scattering rate.

5 Conclusion

In this paper, we have calculated the interface phonon assisted scattering rates in DQW structures. The wave function was calculated by solving the Schrödinger equation coupled with the Poisson equation. The nonparabolic effect is included by the Kane-type dispersion. The interface phonon modes were calculated using the transfer matrix method. It is found that the life time (inverse transition rate) can be very short, less than one picosecond. The interface phonon scattering is therefore very effective to help to achieve population inversion. The scattering rate is sensitive to the quantum well structure parameters. Our result may be very useful for choosing an optimized structure parameter for device performance such as in the quantum cascade laser design and simulation.

This work was supported by the Special Funds for Major State Basic Research Project (G20000683 and 2001CCA02800) and the Special Funds for Shanghai Optic Engineering (011661075).

References

1. Z. Jiang, X.-C. Zhang, IEEE J. Quant. Elec. **36**, 1214 (2000)
2. J.C. Cao, H.C. Liu, X.L. Lei, J. Appl. Phys. **87**, 2867 (2000)
3. P. Harrison, R.A. Soref, IEEE J. Quant. Elec. **37**, 153 (2001)
4. J.C. Cao, H.C. Liu, X.L. Lei, A.G.U. Perera, Phys. Rev. B **63**, 115308 (2001)
5. D. Hashimshony, A. Zigler, D. Papadopoulos, Phys. Rev. Lett. **86**, 2806 (2001)
6. R. Köhler, A. Tredicucci, F. Beltram, H.E. Beere, E.H. Linfield, A.G. Davies, D.A. Ritchie, R.C. Iotti, F. Rossi, Nature **417**, 156 (2002)
7. M. Rochat, L. Ajili, H. Willenberg, J. Faist, H. Beere, G. Davies, E. Linfield, D. Ritchie, Appl. Phys. Lett. **81**, 1381 (2002)
8. O. Gauthier-Lafaye, F.H. Julien, S. Cabaret, J.M. Lourtioz, G. Strasser, E. Gornik, M. Helm, P. Bois, Appl. Phys. Lett. **74**, 1537 (1999)
9. H.C. Liu, I.W. Cheung, A.J. SpringThorpe, C. Dharma-wardana, Z.R. Wasilewski, D.J. Lockwood, G.C. Aers, Appl. Phys. Lett. **78**, 3580 (2001)
10. H.B. Teng, J.P. Sun, G.I. Haddad, M.A. Stroscio, SeGi Yu, K.W. Kim, J. Appl. Phys. **84**, 2155 (1998)
11. M.A. Stroscio J. Appl. Phys. **80**, 6864 (1990)
12. C. Sirtori, F. Capasso, J. Faist, Phys. Rev. B **50**, 8663 (1994)
13. D.F. Nelson, R.C. Miller, D.A. Kleinman, Phys. Rev. B. **35** 7770 (1987)
14. R. Chen, D.L. Lin, T.F. George, Phys. Rev. B **41**, 1435 (1990)
15. H. Rücker, E. Molinari, P. Lugli Phys. Rev. B **44**, 3463 (1991)
16. SeGi Yu, K.W. Kim, M.A. Stroscio, G.J. Iafrate, J.P. Sun, G.I. Haddad, J. Appl. Phys. **82**, 3363 (1997)
17. P. Bordone, P. Lugli, Phys. Rev. B **49**, 8178 (1994)